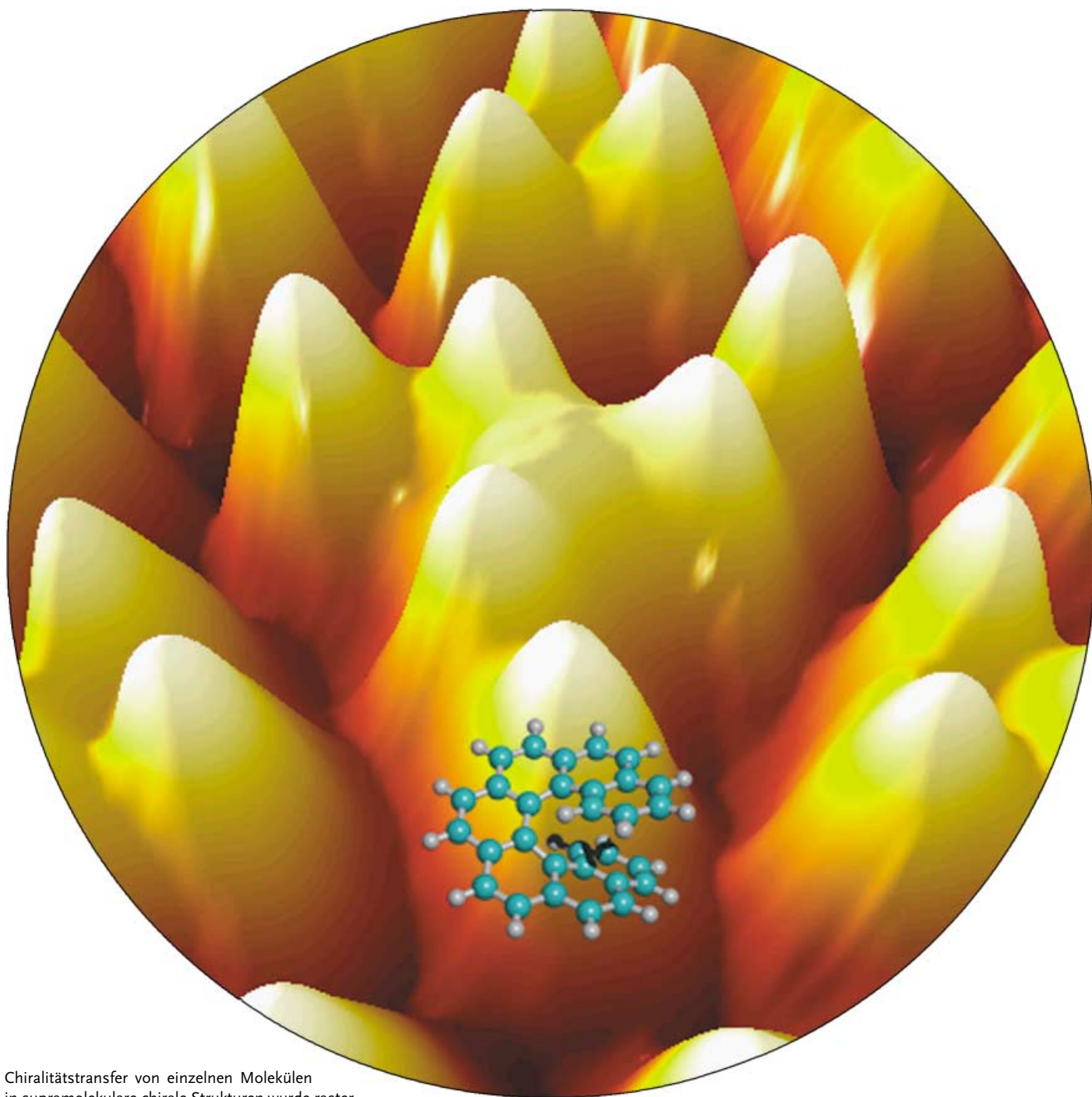# *Zuschriften*

Chiralitätstransfer von einzelnen Molekülen in supramolekulare chirale Strukturen wurde raster-tunnelmikroskopisch untersucht. Jeder „Gipfel" repräsentiert ein (*M*)-Heptahelicen-Molekül auf einer Kupfer(111)-Oberfläche. Der „Gebirgs-zug" im Zentrum besteht aus sechs Molekülen, die eine im Gegenuhrzeigersinn verzerrte Struktur bilden. Mehr hierzu erfahren Sie in der Zuschrift von Fasel, Ernst und Parschau auf den folgenden Seiten.

Chirality Transfer from Single Molecules into Self-Assembled Monolayers**

Roman Fasel,* Manfred Parschau, and Karl-Heinz Ernst*

Self-organization of chiral molecules into helical architectures is of fundamental importance in nature.[1] In addition, interest in the transfer of chirality from single molecules into mesoscopic chiral ensembles is based on its application in liquid-crystal (LC) technologies.[2] The mechanism of chirality induction, that is, the process in which the molecular chirality is mapped onto a supramolecular ensemble, however, is still unclear. The type of intermolecular forces involved in the transfer include hydrogen bonding, π–π interactions, covalent bonding, van der Waals and electrostatic interactions.[3] It has also been predicted by Monte Carlo simulations that steric interaction under influence of repulsive forces alone is sufficient to explain the induction of mesoscopic chirality.[4] Nevertheless, molecular simulations of mesoscopic ensembles based on the structure of the single molecule are computationally very intensive and require either a limit on the number of molecules or greatly simplified molecular shapes.[4]

A promising approach for gaining insight into the process of intermolecular chirality transfer is the investigation of the self-assembly of chiral molecules on solid surfaces, where the chirality transfer is limited to two dimensions. In particular, this allows the use of scanning tunneling microscopy (STM) which is an excellent tool for studying molecular pattern formation.[5] Two-dimensional (2D) chiral effects, such as the spontaneous separation of enantiomers, have also been observed for chiral amphiphiles at the air–solution interface by grazing incidence X-ray diffraction.[6] STM studies of molecular layers adsorbed on well-ordered substrates, however, revealed other forms of expression of chirality in 2D systems, such as the formation of homochiral domains showing opposite angles with respect to a substrate lattice vector[7] and the formation of handed nanostructures.[8] Herein, we report on the mechanism of chirality transfer from helical heptahelicene molecules ([7]H, $C_{30}H_{18}$) into the close-packed monomolecular layer. Under these conditions, that is, when the molecules are squeezed together, repulsive forces dominate the lateral interaction. The self-assembly of molecules on surfaces, however, is not only governed by the lateral interaction between the molecules, but is also influenced by the molecule–substrate interaction, which, in turn, determines the mobility of the molecular species at a given temperature. On Ni(111) and Ni(100), the low mobility of [7]H did not allow the observation of chiral effects.[9] Therefore, we studied the pattern formation on the Cu(111) surface, where at coverages below 95% of the saturated monolayer the molecules are observed to diffuse readily even at lower temperatures.[10] The absence of close-packed structures up to very-high coverages is not unexpected for [7]H since the molecule has no chemical groups capable of directional intermolecular bonding. Therefore, the attractive intermolecular forces are expected to be very weak. At close to full monolayer coverage, [7]H molecules are, however, forced into well-ordered arrangements. The adsorption of racemic [7]H led to the formation of enantiomorphous mirror domains, in which the enantiomers are partially separated.[10] Depending on the enantiomeric excess, the local structures in those domains exhibited minute differences. Herein, however, we focus on the enantiopure structures, in which the expression of chirality goes beyond the formation of mirror domains. Figure 1 shows STM images of the two close-packed
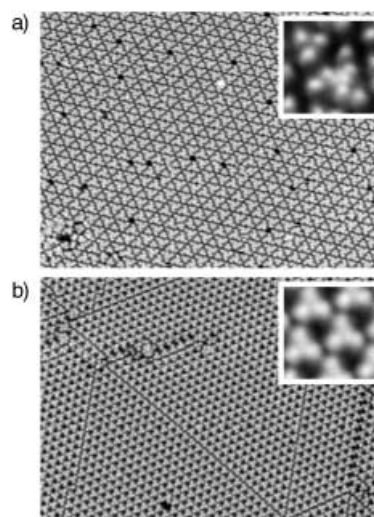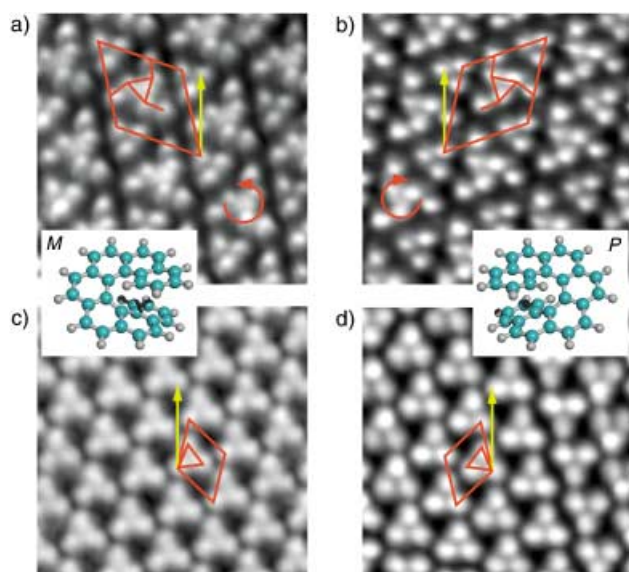

Figure 1. Constant-current STM images (70 nm × 70 nm) acquired at 50 K of long-range ordered monolayers of (*M*)-heptahelicene on Cu(111). a) The 6&3-structure at 95% ($\theta = 0.95$) of the saturated monolayer coverage. b) The 3-structure of the complete monolayer ($\theta = 1$). The insets show the molecular cluster units of the structures.

structures observed for *(M)*-heptahelicene. Each bright dot represents one molecule. At 95% ($\theta = 0.95$) of the monolayer saturation coverage, a long-range ordered structure—apparently built-up from clusters containing six molecules and from clusters containing three molecules ("6&3-structure")—is observed. The six-membered clusters appear as an anticlockwise pinwheel, thus showing handedness. At monolayer saturation coverage ($\theta = 1$) the unit cell of the adsorbate lattice contains a group of three molecules ("3-structure") which appear a particular cloverleaf shape. Two rotational domains, rotated by 180° with respect to each other, are observed in both structures.

[*] Dr. R. Fasel, Dr. K.-H. Ernst, Dr. M. Parschau
Molecular Surface Technologies
Swiss Federal Laboratories for Materials Testing and Research (EMPA)
Ueberlandstrasse 129, 8600 Dübendorf (Switzerland)
Fax: (+41) 1-823-4034
E-mail: roman.fasel@empa.ch
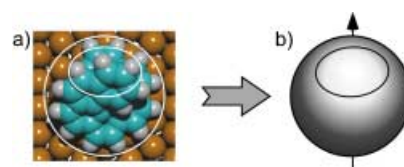   karl-heinz.ernst@empa.ch

The observed adsorbate lattice structures show enantiomorphism, that is, adsorption of the *(P)*-enantiomer of heptahelicene leads to structures which are mirror images of those observed for *(M)*-heptahelicene (Figure 2). Furthermore, the enantiomeric lattices form opposite angles with

Figure 3. Topographic model used for the interpretation of the observed STM images: The [7]H molecule, as adsorbed on Cu(111) (a), is approximated by a disk with a bright protrusion at the topmost part of the molecule (b). The azimuth of a protrusion pointing towards the "12-o'clock" direction is defined as 0°.

Figure 2. High-resolution STM images of (*M*)- and (*P*)-[7]H structures (10 nm × 10 nm). a) (*M*)-[7]H at $\theta = 0.95$. b) (*P*)-[7]H at $\theta = 0.95$. c) (*M*)-[7]H at $\theta = 1$. d) (*P*)-[7]H at $\theta = 1$. The (*M*)- and (*P*)-[7]H structures are mirror images of each other. Unit cells and their basic building blocks are outlined by red lines, the [1 1̄ 0] surface direction is indicated by the yellow arrows.

metry of the topmost Cu(111) layer allows six equivalent azimuthal orientations for the [7]H molecules.[11] These orientations are obtained from the 0° (i.e. "12 o'clock") orientation shown in Figure 3 by successive rotations of 60° about the surface normal, resulting in "10 o'clock", "8 o'clock", …, 2 o'clock orientations. Assuming hexagonal packing and attributing one of the six particular azimuthal orientations to each molecule, both structures can be rationalized within this simple picture (Figure 4). Going
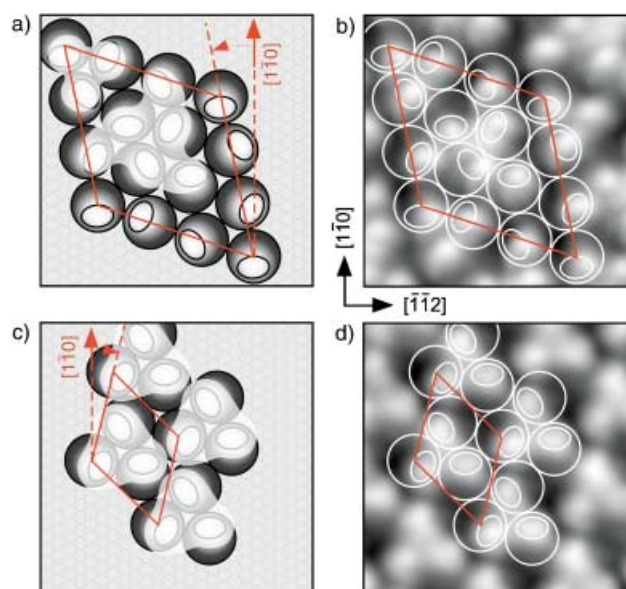
respect to the [1 1̄ 0] substrate surface direction. Since the angle between the adsorbate and substrate-surface lattice vectors is oblique, the supramolecular assembly breaks the symmetry of the underlying substrate surface. The combined molecule–substrate systems thus exhibit extended surface chirality. Remarkably, the unit cells are not only mirror images of each other, but also the arrangements of molecules within the unit cells. This is most clearly seen for the pinwheel-clusters of the 6&3-structures (Figure 2a and b): The pinwheel's wings point either anticlockwise, as in the *(M)*-heptahelicene 6&3-structure, or clockwise, as in the *(P)*-heptahelicene 6&3-structure. In the case of the 3-structures (Figure 2c and d), the mirror symmetry is expressed by tilts of the three-molecule cloverleaf units into opposite directions with respect to the adsorbate lattice vectors.

To interpret the observed handed supramolecular structures, we make use of the following simple topographic model: Based on the assumption that the brightest feature in the constant-current STM image corresponds to the uppermost part of the molecule, the [7]H molecule is approximated by a disk with an off-center protrusion (Figure 3). The adsorption geometry depicted in Figure 3 derives from a previous X-ray photoelectron diffraction (XPD) study where we showed that [7]H is adsorbed with a terminal phenanthrene group parallel to the Cu(111) surface.[11] The XPD experiments also confirmed that the sixfold rotational sym-

Figure 4. Structure models for the (*M*)-heptahelicene 6&3-molecule cluster (a and b) and the (*M*)-heptahelicene 3-molecule cluster structures (c and d) based on a hexagonal packing of the molecules and systematically varying azimuthal orientations. The model structures are superimposed on the corresponding STM images in (b) and (d).

anticlockwise along the contour of the six-molecule-pinwheel, the [7]H molecules are rotated by +60° with respect to each other (Figure 4a and b). The three-molecule corner unit of the 6&3-structure is accounted for by [7]H molecules facing each other in an anticlockwise fashion, which corresponds to relative azimuthal orientations of +120°. Similarly, the cloverleaf unit of the 3-structure is due to three molecules oriented 0°, 120°, and 240° (Figure 4c and 4d).

In the framework of this simple model, the symmetry of the close-packed layer is lowered due to the *C*1 symmetry of the adsorbed [7]H molecules and, in addition, because of their

chirality. Consequently, particular combinations of neighboring azimuthal orientations are energetically more favorable than others. This situation leads to a distinct transfer of the structural information—the chirality in our case—into the 2D organized layer. Hence, the chirality is not only expressed by opposite angles of the domains with respect to the substrate, but also by a correlation of azimuthal orientations between neighboring molecules which leads to handed molecular structures. Although the arrangement of the molecules is 2D-quasi-hexagonal, the resulting surface topography, as imaged by STM, is highly anisotropic and exhibits chirality. In previously reported systems either the local molecule–substrate arrangement determined the angle of the chiral domain with respect to the substrate lattice[12] or chiral clusters and nanostructures were created through polar lateral interactions, for example, by hydrogen bonding.[8] In our case, however, it is the shape of the molecule under repulsive conditions that governs the transfer of chirality.

To corroborate this transfer mechanism and to confirm the proposed azimuthal arrangement, we have performed molecular modeling calculations for the monolayer 3-structure.[13] The unit cell considered in these calculations, as determined from a series of STM images, is sketched in Figure 5a. The molecules at the four corners of the unit cell have an identical azimuthal orientation 1 (Figure 5a). For perfectly hexagonal packing, the remaining two molecules,

taking positions 2 and 3, are symmetrically centered within the unit cell, as indicated by the yellow dots in Figure 5a. Owing to the oblique orientation of the adsorbate unit cell with respect to the substrate lattice this results, however, in different adsorption sites for the molecules at positions 2 and 3 than for the corner molecules. Therefore, we have also considered possible lateral shifts of the molecules at positions 2 and 3 to the nearest equivalent adsorption sites, labeled t1, t2, and t3 in Figure 5a. The total energy of the system was calculated for all combinations of adsorption sites (4×4 possibilities) and azimuthal orientations (in steps of 15°). We find two geometries (Figure 5c and d) with equal and lowest total energy. In both geometries, molecules at positions 2 and 3 are shifted away from the central position within their respective unit-cell half way towards one of the corner molecules. Whereas the configuration shown in Figure 5c corresponds to molecules at positions 2 and 3 being shifted onto sites t1 and t3, respectively, the equally favorable configuration shown in Figure 5d is obtained by shifting the molecules with orientations 2 and 3 onto sites t3 and t2, respectively. In both minimum-total-energy configurations the relative azimuthal orientations of the molecules amount to 120°: With respect to the 0° orientation as defined in Figure 3, the azimuthal orientations of the cloverleaf cluster molecules are 60°, 180°, and 300° (Figure 5c), or 0°, 120°, and 240° (Figure 5d). The latter azimuthal orientation angles are clearly identical to those derived from the topographic modeling of the STM image as shown in Figure 4c and d, thus confirming our structure model. Remarkably, the two total-minimum-energy configurations of the calculation are both experimentally observed as rotational domains of the 3-structure: Whereas the 0°–120°–240° minimum-energy configuration (Figure 5d) corresponds to domain d2 (Figure 5b), domain d1 is formed by molecules taking 60°–180°–300° azimuthal orientations as shown in Figure 5c.

Although total energies determined from AMBER force-field calculations can not be taken as absolute values, relative energies should accurately reflect the energetics of different supramolecular arrangements. We find that a single [7]H molecule adsorbed at an on-top site on Cu(111) is 1 eV lower in energy than within the close-packed 3-structure. Packing of [7]H into the 3-structure thus costs about 1 eV per molecule, which reflects the rather strong repulsive intermolecular interaction. Therefore, the molecules take the particular azimuthal orientations that minimize the repulsive interactions between them.

For rigid molecules adsorbed on a surface, the optimization of relative azimuthal orientations is the only way to minimize the lateral pressure to some extent. In monolayers of chiral LC-like molecules with long alkyl chains, repulsion causes the chains to bend partly away from the surface.[14] In such cases, the expression of chirality is limited to the formation of lamella structures forming mirror domains. The 2D orientation mechanism observed in our system can be considered as the analogue of the helical twisting in 3D cholesteric phases. The very high twisting power (TP) of bridged biaryl compounds in biphenyl nematics, for instance, has been assigned to the rigid helical part rather than the long alkyl chains.[15] This mechanism of chirality induction has
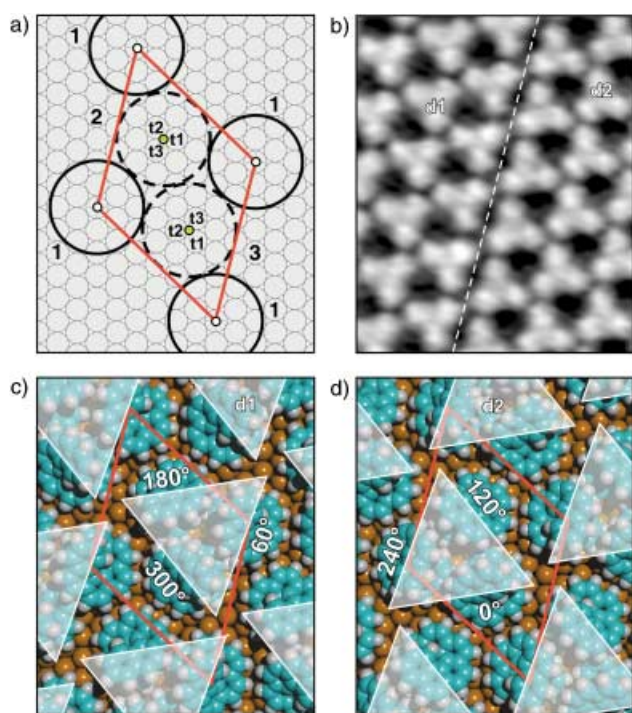
Figure 5. Molecular modeling results compared to STM results of the 3-structure at saturated monolayer coverage. a) Adsorption sites within the unit cell considered for the calculations. b) STM image of a domain boundary (dashed line) between the two rotational domains d1 and d2. c) and d) The two lowest total-energy configurations as determined from the calculations. White semi-transparent triangles highlight the topmost parts of the molecules that are imaged brightest. Both geometries are in excellent agreement with the observed d1 and d2 domain structures.

been supported by theoretical predictions of the TP within the so-called surface model.[16] Similar conclusions have been drawn from Monte Carlo simulations on model mesogens by Selinger and co-workers.[4] This shows that surface studies of 2D model systems are an excellent approach towards an understanding of the far more complicated 3D LC systems.

In summary, ordered supramolecular chiral structures have been observed after deposition of pure heptahelicene enantiomers on Cu(111). Besides showing opposite angles between the enantiomorphic adsorbate lattices and the substrate lattice, long-range chirality is also expressed by opposite tilt angles of molecular clusters with respect to the adsorbate lattice vectors, and by formation of handed molecular clusters. We have shown that the chirality transfer occurs through steric repulsion and does not require molecular flexibility or strong dipole interactions. The appearance of handed molecular clusters is due to a correlation of azimuthal molecular orientations which are driven by repulsive intermolecular forces in the close-packed 2D layer.

Experimental Section

Heptahelicene was synthesized as described elsewhere.[17] Enantiomeric separation ($ee > 99.9\%$) was accomplished by HPLC on a Daicel Chiracel OD column and subsequently tested by HPLC using a Chiracel OD-H column. Assignment of the enantiomers was based on circular dichroism (CD) spectra in accordance to Martin and Marchant.[18] The molecules were evaporated in ultrahigh vacuum (UHV) from a Knudsen-cell type evaporator, held at 150 K during deposition onto the clean Cu(111) substrate which was held at room-temperature. The Cu(111) surface was prepared by repeated cycles of Ar$^+$ sputtering and annealing to 800 K. After cooling of the sample to 50 K, STM images were acquired in constant-current mode. Molecular modeling was performed using the AMBER force field of the Hyperchem 7 package.[19]

[1] A. E. Rowan, R. J. M. Nolte, *Angew. Chem.* **1998**, *110*, 65–71; *Angew. Chem. Int. Ed.* **1998**, *37*, 63–68, and references therein.

[2] a) H.-G. Kuball, T. Höfer in *Chirality in Liquid Crystals* (Eds.: H.-S. Kitzerow, C. Bahr), Springer, New York, **2001**, pp. 67–100; b) R. P. Lemieux, *Acc. Chem. Res.* **2001**, *34*, 845–853.

[3] a) H. Engelkamp, S. Middelbeek, R. J. M. Nolte, *Science* **1999**, *284*, 785–788, and references therein; b) S. Kirstein, H. von Berlepsch, C. Bötticher, C. Burger, A. Quart, G. Reck, S. Dähne, *ChemPhysChem* **2000**, *1*, 146–150.

[4] J. Xu, R. L. B. Selinger, J. V. Selinger, R. Shashidhar, *J. Chem. Phys.* **2001**, *115*, 4333–4338.

[5] a) J. Rabe, S. Bucholz, *Science* **1991**, *253*, 424–427; b) J. S. Forster, J. E. Frommer, *Nature* **1988**, *333*, 542–545; c) J. Frommer, *Angew. Chem. Int. Ed. Engl.* **1992**, *31*, 1298–1328; *Angew. Chem.* **1992**, *104*, 1325.

[6] I. Weisbuch, I. Kuzmenko, M. Berfeld, L. Leiserowitz, M. Lahav, *J. Phys. Org. Chem.* **2000**, *13*, 426–434.

[7] a) F. Stevens, D. J. Dyer, D. M. Walba, *Angew. Chem. Int. Ed. Engl.* **1996**, *35*, 900–901; *Angew. Chem.* **1996**, *108*, 955–957; b) S. De Feyter, A. Gesquire, K. Wurst, D. B. Amabilino, J.

Veciana, F. C. De Schryver, *Angew. Chem.* **2001**, *113*, 3317–3320; *Angew. Chem. Int. Ed.* **2001**, *40*, 3217–3220; c) S. De Feyter, A. Gesquire, F. C. De Schryver, C. Meiners, M. Sieffert, K. Müllen, *Langmuir* **2000**, *16*, 9887–9894; d) Q.-M. Xu, D. Wang, L.-J. Wan, C. Wang, C.-L. Bai, G. Q. Feng, M.-X. Wang, *Angew. Chem.* **2002**, *114*, 3558–3561; *Angew. Chem. Int. Ed.* **2002**, *41*, 3408–3411.

[8] a) M. Böhringer, K. Morgenstern, W.-D. Schneider, R. Berndt, *Angew. Chem.* **1999**, *111*, 832–834; *Angew. Chem. Int. Ed.* **1999**, *38*, 821–823; b) M. Böhringer, W.-D. Schneider, R. Berndt, *Angew. Chem.* **1999**, *111*, 832–834; *Angew. Chem. Int. Ed.* **2000**, *39*, 792–795; c) J. V. Barth, J. Weckgesser, C. Cai, P. Günter, L. Bürgi, O. Jeandupeux, K. Kern, *Angew. Chem.* **2000**, *112*, 1285–1288; *Angew. Chem. Int. Ed.* **2000**, *39*, 1230–1234.

[9] K.-H. Ernst, Y. Kuster, R. Fasel, C. F. McFadden, U. Ellerbeck, *Surf. Sci.* **2003**, *530*, 195–202.

[10] a) K.-H. Ernst, Y. Kuster, R. Fasel, M. Müller, U. Ellerbeck, *Chirality* **2001**, *13*, 675–678; b) M. Parschau, R. Fasel, K.-H. Ernst, unpublished resutls.

[11] R. Fasel, A. Cossy, K.-H. Ernst, F. Baumberger, T. Greber, J. Osterwalder, *J. Chem. Phys.* **2001**, *115*, 1020–1027.

[12] J. V. Barth, J. Weckesser, G. Trimarchi, M. Vladimirova, A. de Vita, C. Cai, H. Brune, P. Günter, K. Kern, *J. Am. Chem. Soc.* **2002**, *124*, 7991–8000, and references therein.

[13] Because many more parameters need to be considered for the 6&3-structure, molecular mechanics calculations of this structure are too extensive. However, the same mechanism of minimization of repulsive interactions for a given unit-cell size and occupation should hold true also in that case.

[14] a) F. Stevens, D. J. Dyer, U. Müller, D. M. Walba, *Langmuir* **1996**, *12*, 5625–5629; b) S. De Feyter, A. Gesquière, P. C. M. Grim, F. C. De Schryver, S. Valiyaveetil, C. Meiners, M. Sieffert, K. Müllen, *Langmuir* **1999**, *15*, 2817–2822.

[15] G. Gottarelli, M. Hilbert, B. Samori, G. Solladié, G. P. Spada, R. Zimmerman, *J. Am. Chem. Soc.* **1983**, *105*, 7318–7321; b) G. Gottarelli, G. P. Spada, R. Bartsch, G. Solladie, R. Zimmerman, *J. Org. Chem.* **1986**, *51*, 589–592; c) G. Gottarelli, G. Proni, G. P. Spada, D. Fabbri, C. Rosini, *J. Org. Chem.* **1996**, *61*, 2013–2019.

[16] a) A. Ferrarini, P. L. Nordio, *J. Chem. Soc. Perkin Trans. 2* **1998**, *2*, 455–460; b) A. Ferrarini, G. J. Moro, P. L. Nordio, *Mol. Phys.* **1996**, *87*, 485–499.

[17] A. Sudharkar, T. J. Katz, *Tetrahedron Lett.* **1986**, *27*, 2231.

[18] R. H. Martin, M. J. Marchant, *Tetrahedron* **1974**, *30*, 347.

[19] HyperChemRelease7, Hypercube Inc., (http://www.hyper.com/) **2002**.